Divertor radiation distribution during ELMs in JET

A. Huber[1]**,** R. A. Pitts[2], V. Philipps[1], A. Loarte[3], P. Andrew[4]**,** S. Brezinsek[1], J. P. Coad[4],
W. Fundamenski[4], S. Jachmich[5], A. Korotkov[4], J. Marki[2], G.F. Matthews[4], K.McCormick[6],
Ph. Mertens[1], J. Rapp[1], G. Sergienko[1], M. Stamp[4] and JET EFDA contributors*

[1]*Institut für Energieforschung-Plasmaphysik,, Forschungszentrum Jülich GmbH, EURATOM
Association, Trilateral Euregio Cluster, D-52425 Jülich, Germany, www.fz-juelich.de/ief/ief-4*
[2]*CRPP, Association EURATOM-Confédération Suisse, EPFL, Lausanne, Switzerland*
[3]*EFDA Close Support Unit – Garching, Boltzmannstrasse 2, D-85748 Garching, Germany*
[4]*Euratom/UKAEA Fusion Association, Culham Science Centre, Abingdon, Oxon OX14 3DB, UK*
[5]*Laboratory for Plasmaphysics, ERM/KMS, Association EURATOM-Belgian State, Brussels, Belgium*
[6]*Max-Planck-Institut für Plasmaphysik, EURATOM Association, 85748 Garching, Germany*
**See the Appendix of M.L. Watkins et al., Fusion Energy 2006(Proc. 21st Int. Conf. Chengdu, 2006) IAEA, (2006)*

Introduction. The Type I ELMy H-mode regime is the baseline scenario for operation of ITER in high fusion gain regimes ($Q_{DT} \geq 10$) with high density plasmas ($<n_e> \geq 10^{20} m^{-3}$) and with high plasma energy (~350 MJ) [1]. The major drawback of this operating regime is the ELM-associated periodic power loading of plasma-facing components which can lead to high target erosion and a significant reduction of component lifetimes. In present tokamaks, the plasma energy drop normalised to the pedestal energy, $\Delta W_{ELM}/W_{ped}$ during a Type I ELM is typically 3-10%. A significant part of this energy can be found in form of plasma radiation, located mostly in the divertor region (in the present contribution, it is integrated over ~2ms, which is considerably longer than the ELM target power deposition of several 100 μs). Systematic studies of the distribution and magnitude of this radiation are required in order to understand and predict the energy deposition by ELMs on plasma-facing components in larger devices such as ITER, where even the smallest Type I ELMs will considerably exceed the maximum energies currently accessible.

Experimental set-up Dedicated experiments aiming at the characterisation of transient loads during large Type I ELMs have been performed during the 2007 JET campaigns at high plasma current and input power: I_p=3.0 MA, B_T=3.0 T, q_{95}=3.2, δ_u~0.22, δ_l~0.28, κ=1.73, 19 MW NBI and 1.4 MW ICRH power. The JET bolometer camera system has recently been substantially upgraded, allowing significantly improved spatial and temporal resolution of the radiation distribution, particularly in the divertor region [2]. This allows a greatly improved tomographic reconstruction of the radiation pattern on a timescale of the order of the typical duration of a Type I ELM cycle (~ 1

Fig.1 #70226: discharge overview: I_p=3.0MA, B_T=3.0T, δ_l~0.28, vertical target

ms). In addition, the new system permits for the first time on JET an accurate analysis of the total energy radiated by any particular ELM, even in the case of smaller, higher frequency Type III ELMs.

Results and Discussion The gas fuelling has been varied in a series of repeated 3.0 MA discharges to produce Type I ELMs of different sizes ($\Delta W_{ELM}/W_{ped}$ increases with decreasing gas fuelling) in the ELM energy range ΔW_{ELM} =0.2→0.9MJ. Fig. 1 shows typical time traces of the parameters of an ELMy H-mode discharge in JET with strike points located on the lower vertical tiles of the MkII-HD divertor for a discharge without gas fuelling, with large (giant) ELMs ($\Delta W_{ELM} \approx$0.9MJ). Such ELMs are often followed by a phase of Type III ELMs or even a brief return to L-mode confinement. The

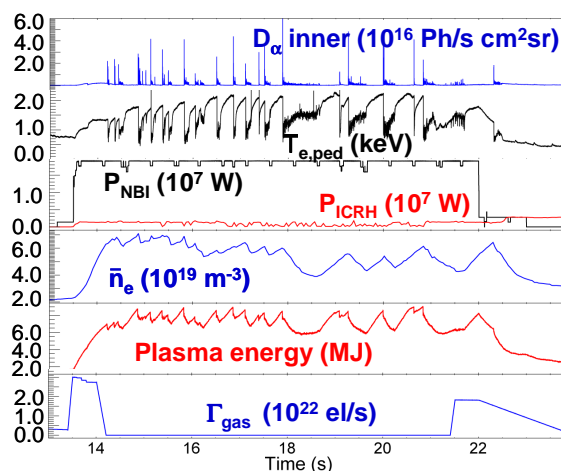"global energy balance" for this discharge (energy balance integrated over the entire discharge) reads:

total injected energy of E_{in}=177MJ, radiated energy E_{rad}=82.4MJ, E_{rad}/E_{in}=0.47 and deposited energies onto inner and outer divertor targets of 24.6MJ and 70.9MJ respectively. Despite the large influence of the gas fuelling on the ELM behaviour, the global energy balance shows negligible variations with different gas levels and correspondingly with different ELM sizes.

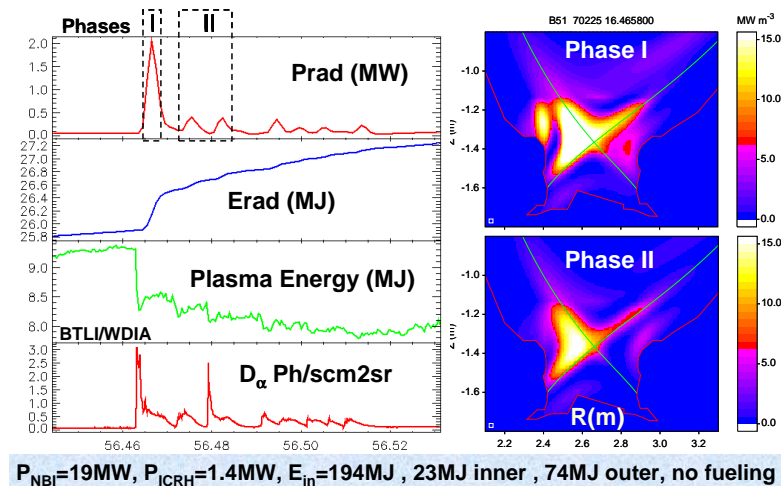**P_{NBI}=19MW, P_{ICRH}=1.4MW, E_{in}=194MJ , 23MJ inner , 74MJ outer, no fueling**

Fig.2 Typical large ELM radiation distribution

Fig.2 shows the divertor radiation distributions integrated over two different phases during a large ELM with ΔW_{ELM}~ 0.9 MJ. The first phase, of ~ 4 ms duration includes radiation during the ELM crash and the second (~ 14 ms) during the Type III ELM compound phase which follows. The left side of the figure shows the total power, stored energy, radiated energy, and inner divertor D_{α}-emission. The time intervals (phases I and II) in the shaded regions delimit the time over which the bolometry signals have been averaged.

In both phases the radiation distribution is strongly weighted to the inner divertor region (in-out asymmetries of ~factor 3 in phase I). This is also the case during the inter-ELM period, but with a lower asymmetry factor of ~2. This reflects the higher density, cooler plasma at the inboard divertor for forward toroidal field operation. The total radiated energy during the Type I ELM, evaluated by an algorithm similar to that described in [3], is 570kJ,
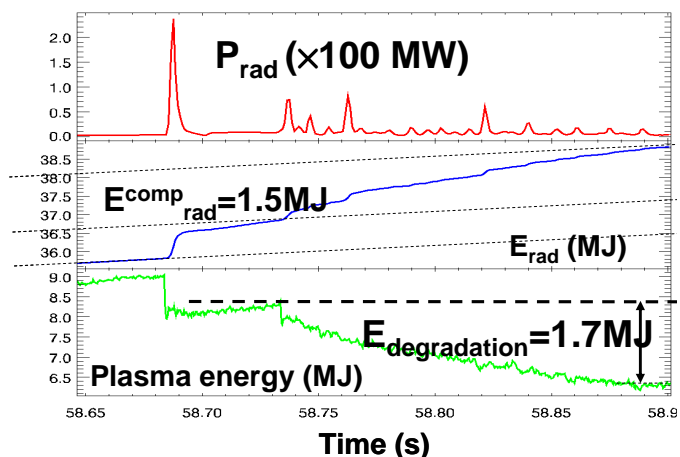

Fig.3 Calculation of the radiated energy during the „compound"phase of the ELM.

corresponding to 72% of the ELM-energy losses (ΔW_{ELM} ≈790kJ). It is important to note that that the radiated power is determined by the radiation from the particle release due to the ELM-target interaction together with the changes in the local plasma parameters provoked by the ELM.

Along with the critical question of the radiated energy during the Type I phase, the radiated energy during the compound phase is an important parameter. Fig. 3 illustrates the strong degradation of the plasma energy during the compound phase; analysis of the radiation occurring during this phase shows that it accounts for a significant fraction (up to 90%) of the plasma energy loss.

Fig. 4 presents the dependence on ΔW_{ELM} of the radiated plasma energy following the ELM crash. Here the radiated energy contains only the part of the radiated losses which occurs during the first main peak during the ELM. For an ELM energy below about 700kJ, the radiated plasma energy is proportional to the ELM energy, as expected from the observed linear correlation between impurity influxes and ELM sizes. In this range the ELMs radiates ~50% of the ELM energy drop.

Beyond a ΔW_{ELM} of ~700 kJ, a non-linear increase of the divertor radiation occurs which is interpreted as an indication of additional carbon evolution from the target tiles, possibly due to material ablation. The target surface temperature during the transient loads as measured with infra-red thermography reaches peak values of ~2000°C at the inner divertor and only ~800°C at the outer. Even the maximum value is too low for bulk carbon ablation which would correspond to a carbon sublimation of about 10^{19} C/m^2 s at this temperature, yielding a total release of 2×10^{19} C/ s for a 0.5m^2 loaded surface during the ELM. This quantity of carbon is much smaller
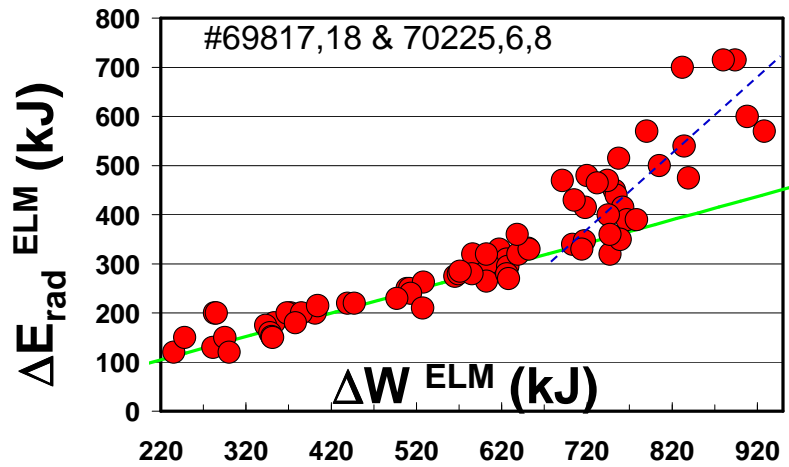
Fig.4 Radiated Plasma energy following Type I ELMs versus ELM energy loss

than the known intrinsic carbon sources (~ 10^{21} C/ s from the main wall and ~7×10^{21} C/ s from the divertor [4]). The enhanced radiation losses over ΔW_{ELM} ~700 kJ can almost certainly be explained by the ablation of the re-deposited carbon layer which is known to exist on the inner divertor target. The inner divertor is always a region of net deposition on JET and the outer of net erosion for standard forward field operation [5]. These layers with poor thermal contact and low thermal capacity respond much more strongly to the power flux than the bulk target tiles. The re-deposited layers in the inner divertor contain a large amount of Be ($\approx$50%). Interestingly, the fast signals in BeII- and CIII-emission react at the same time (~300µs after fall in plasma energy) during the transient events, confirming the assumption of ablation of deposited layers in the inner divertor.

As mentioned above, the inter-ELM radiation distribution is always strongly weighted to the inner divertor volume (in-out asymmetries of ~factor 2). The ELM exacerbates this radiation asymmetry, with the magnitude of the increase linearly dependent on the ELM energy in the range ΔW_{ELM} ~100 -

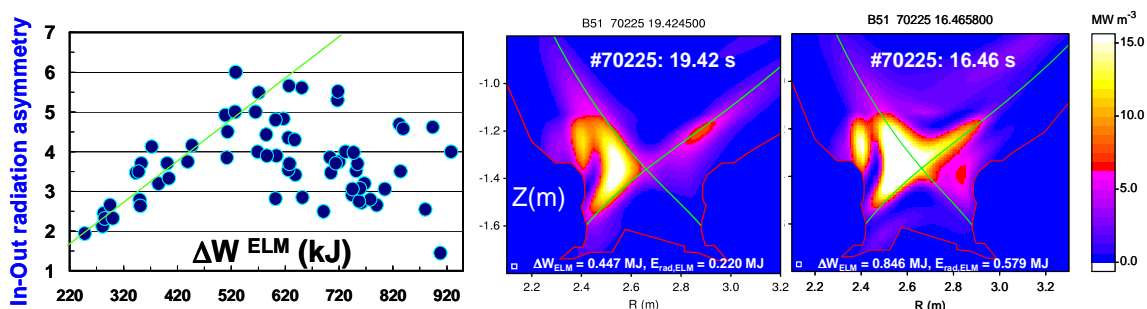Fig.5. In-Out radiation asymmetry versus ELM energy loss and radiation reconstructions for medium and high ΔW_{ELM}.

600 kJ (see Fig.5). This is consistent with fast infrared thermography of the divertor targets which finds that Type I ELMs deposit twice as much energy at the inner target than at the outer across the whole range of Type I ELM energies currently accessible (ΔW_{ELM}= 0.1 – 1.0 MJ) [6]. For ΔW_{ELM} >620kJ the in-out asymmetry shows a "break" in the linear dependence. One explanation for this observation is the assumption that ablated material can reach the outer divertor via the private flux region and thus contribute to the radiation in the outer divertor volume. Secondary peaks on fast CIII divertor spectroscopy with ~0.5 ms delay compared with the first peak at the outer divertor confirm

this assumption. This time delay is approximately equal to the divertor transit time for thermal carbon atoms and C_2 molecules. Additionally, Fig. 5 (right) shows the radiation distribution for ELMs with
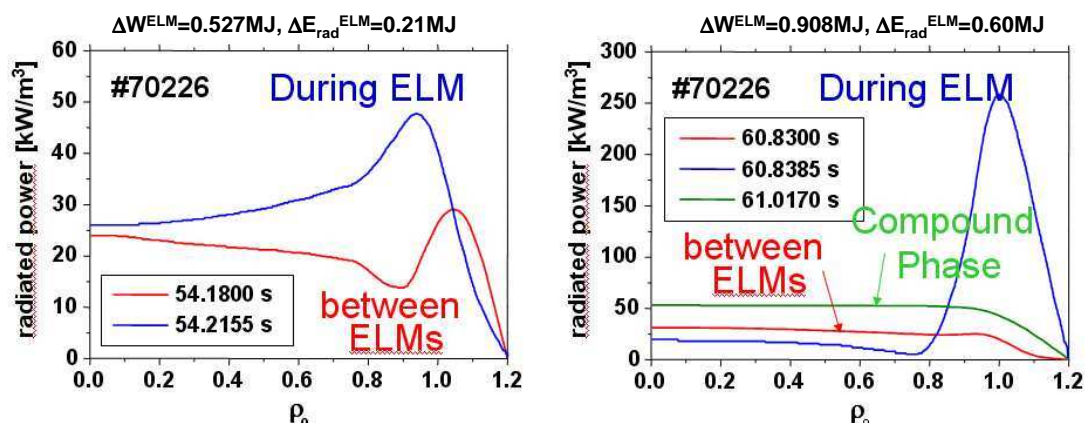

Fig. 6 Radiative profiles for ELMs with medium and large sizes

medium and large sizes. For large ELMs the radiation "spills over" into the outboard X-point region. The impurity influxes associated with transient events can have a significant influence on the discharge since they can lead to an increased plasma contamination and even to a radiative collapse. Fig. 6 shows the radiation profiles for ELMs with medium (left figure) and large (on the right) sizes. This analysis shows a strong increase of the radiation in the edge (normalised minor radius $\rho > 0.8$) during the largest events in the database. The profile during the "compound" phase clearly shows increased radiation in the plasma core and correspondingly points to an increased plasma contamination. An increase of Z_{eff} by about $\Delta Z_{eff} \approx 0.4$-$0.5$ has been observed in the compound phase.

Summary and conclusion

- Large ELMs are often compound (Type I ELM followed by Type III ELMs).

- A significant fraction (up to 90% of radiated energy integrated over the compound phase) of the plasma energy degradation during the compound phase is exhausted by radiation.

- About ~50% of ΔW_{ELM} is radiated in the ELM energy range between 0.1MJ and 0.9MJ.

- Large type I ELMs with energy losses above 0.7MJ show enhanced radiation losses, almost certainly associated with ablation of a re-deposited carbon layer in the inner divertor.

- ELM-induced radiation is always higher at the inner than at the outer divertor: this asymmetry increases approximately linearly to $\Delta W_{ELM} \sim 0.6$ MJ, then decreases for higher ΔW_{ELM}.

- The higher inner divertor radiation is consistent with (but not only due to) a higher ELM energy deposition at the inboard side observed with IR thermography.

- Surface (layer) temperatures do not exceed ~ 2000°C at the inner target. The maximum outer target temperature amounts to ~ 800 °C (no layers). In neither case is the surface temperature sufficient for bulk carbon ablation to occur.

- During the "compound" phase plasma contamination can increase but does not usually lead to radiative collapse of the plasma.

References

[1] ITER Physics Basis Editors, Nucl. Fusion **39** (1999) 2137

[2] A. Huber, K. McCormick, P. Andrew, et al., Fusion Eng. Design (2007), doi:10.1016/j.fusengdes.2007.03.027

[3] J. C. Fuchs, T. Eich, A. Hermann et al., J. Nucl. Mater. 337-339 (2005) 756

[4] J. D. Strachan, W. Fundamenski, M. Charlet et al., Nuclear Fusion 43 (2003) 922

[5] J. P. Coad et. al., Nuclear Fusion 46 (2006) 350

[6] T. Eich et al., J. Nucl. Matter. 363-365 (2007) 989